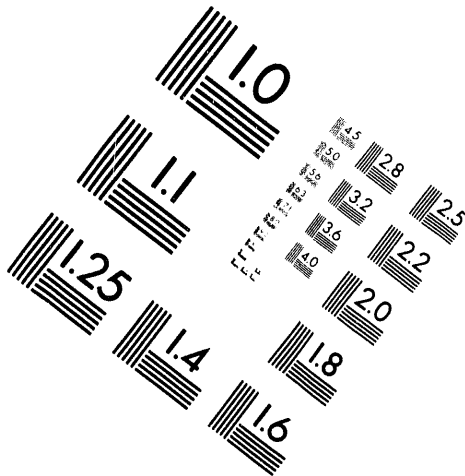
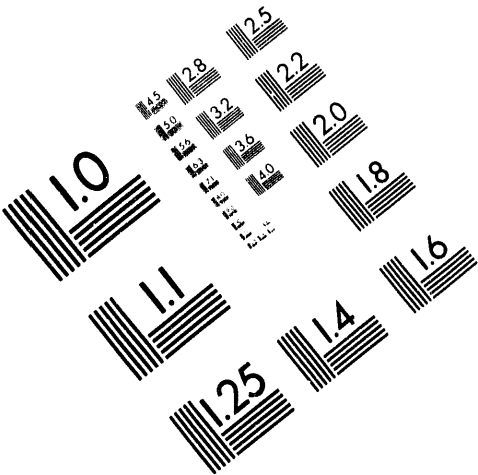




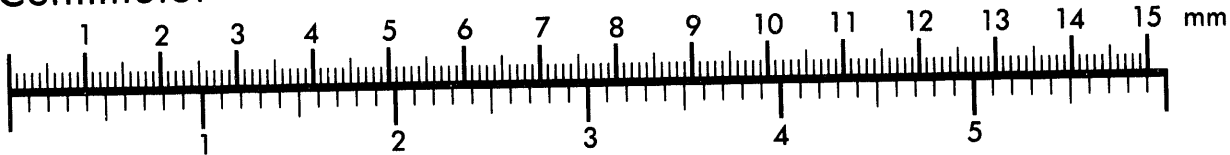
**AIM**

**Association for Information and Image Management**

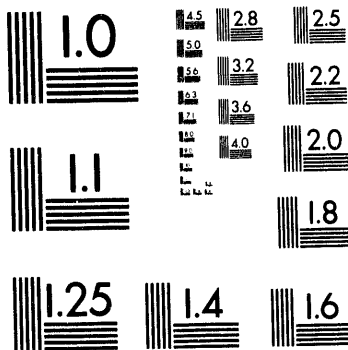
1100 Wayne Avenue, Suite 1100  
Silver Spring, Maryland 20910  
301/587-8202



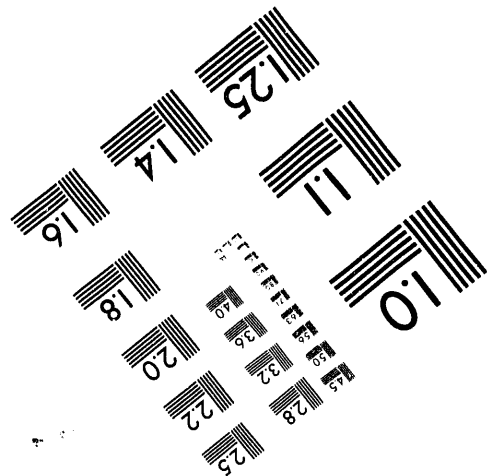
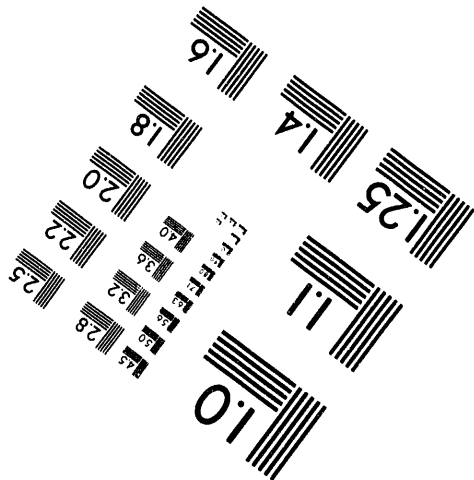
Centimeter



Inches



MANUFACTURED TO AIM STANDARDS  
BY APPLIED IMAGE, INC.



**1 of 1**

SAND -- 94-...  
Conf. 940859 -- 25

## Optimal Trajectories for Flexible-Link Manipulator Slewing Using Recursive Quadratic Programming: Experimental Verification<sup>1</sup>

Gordon G. Parker  
G. Richard Eisler  
John T. Feddema

Department 1434  
Sandia National Laboratories  
Albuquerque, New Mexico  
(505) 844-8864  
ggparke@sandia.gov

### ABSTRACT

Procedures for trajectory planning and control of flexible link robots are becoming increasingly important to satisfy performance requirements of hazardous waste removal efforts. It has been shown that utilizing link flexibility in designing open loop joint commands can result in improved performance as opposed to damping vibration throughout a trajectory. The efficient use of link compliance is exploited in this work. Specifically, experimental verification of minimum time, straight line tracking using a two-link planar flexible robot is presented. A numerical optimization process, using an experimentally verified modal model, is used for obtaining minimum time joint torque and angle histories. The optimal joint states are used as commands to the proportional-derivative servo actuated joints. These commands are precompensated for the nonnegligible joint servo actuator dynamics. Using the precompensated joint commands, the optimal joint angles are tracked with such fidelity that the tip tracking error is less than 2.5 cm.

### INTRODUCTION

Underground nuclear waste tank cleanup will require remote operation of manipulators entering constrained openings where tank inner diameters will be as large as 21 m (U.S. DOE). Manipulators of interest include multi-link configurations of a folded and/or telescoping nature. Once inside the tank, the manipulators will need to cover the workspace with large angle slewing maneuvers for surveying at first, followed by cleanup operations. The sensor and tool palettes slated as end effectors for these multi-link "boom" manipulators are projected to range in weight from 2000 to 9000 N.

The boom arrangements are inherently flexible due to the need to get sufficient hardware to cover the workspace through a con-

strained opening. The addition of heavy payloads accentuates the problem. Remote operators moving these booms, in a typical servo operation, will be constrained to slow maneuvers to avoid oscillations. Performance of the human or autonomous operated systems is increased by using apriori knowledge of the structural dynamics to determine vibration-suppressed open-loop joint trajectory histories. Vibration due to model uncertainty or external disturbances could be compensated for by an outer loop control system.

In this paper the theoretical study of [Eisler, et. al.] is experimentally verified using a two-link flexible robot. The test case consists of straight line tip tracking using joint angle commands generated by an optimization process. These generated commands utilize the flexibility of the links to accomplish the maneuver. However, the joint actuator servo dynamics are not accounted for in the commands. Therefore, joint angle commands are precompensated using an inverse input/output operator technique.

### EXPERIMENTAL SET-UP

The two-link robot of Figure 1 consists of two flexible aluminum links, two motor amplifiers, two DC servo motors, two joint angle encoders, two joint angle tachometers and a VMEbus computer system. The flexible links are mounted so as not to produce significant deformation in the vertical direction. The motors at joints one and two (referred to as the hub and elbow joints from here on) produce a maximum torque of 7.0Nm and 2.25Nm. Link characteristics are given in Table 1.

A VME-based 68030 computer, encoder counter board, and I/O board are used to control the system. The sampling rate of the 68030 computer is 1000 Hz. Two twelve bit encoder counters measure the angles of the motors. Two twelve bit A/D channels are used to measure the angular velocity of each joint. These angular velocity signals are filtered using a 100 Hz low-pass filter digitally implemented using Euler integration.

<sup>1</sup> Work supported by the U.S. Department of Energy at Sandia National Laboratories under Contract DE-AC04-94AL85000

MASTER

## THE STRUCTURAL MODEL

The equation of motion derivation is described in detail in [Eisler, et. al.], a short description is given here for completeness.

All motion is assumed to occur in the x-y plane as shown in Figure 2. The center of each cross section is identified by its arc length distance from the hub  $s$ . The vector  $\beta(s, t)$  is the unit tangent along the arm at  $s$ , and  $\theta$  is the inertial angle to  $\beta$ .



FIGURE 1. Sandia Flexible Two-Link Robot

angle at node  $m$ ,  $M_{m,n}$  and  $K_{m,n}$  are the mass and stiffness matrices, respectively, and  $\beta_m$  is the unit tangent vector at node  $m$ .

The equations of motion of Eq. (1) are integrated using a Newmark- $\beta$  (Newmark, 1959) method. The solutions of the resulting nonlinear algebraic equations in  $\ddot{\theta}_n$  are obtained with a Newton method.

The model used in (Eisler, et.al., 1993) was updated based on the modal testing of the structure detailed in (Mayes, 1991). However, due to the accuracy of the original model, the updated model gives nearly identical results.

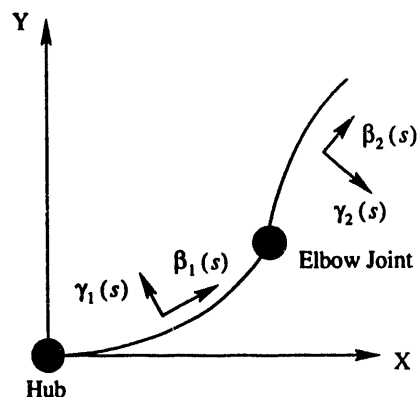


FIGURE 2. Coordinate System Definition

TABLE 1. Link Characteristics

Parameter Name	Unit	Link 1	Link 2
Length	m	0.489	0.463
Height	m	0.762	0.152
Thickness	m	0.00476	0.00159
Young's Mod.	GPa	70	70
Mass Density	kg/m	1.96	1.96

Each flexible link is discretized into three elements, furthermore each rigid link/joint mounting bracket is described by a single element. The elbow joint is described by two collocated nodes so that a nonzero angle is permitted. The constraint of continuous slope between angles is satisfied by the choice of element basis functions. Hamilton's principle is applied to the discretized system after obtaining expressions for kinetic energy, strain energy, and the virtual work due to the applied motor torques. The result is a set of second-order equations in the node unknowns,  $\ddot{\theta}_n$

$$\hat{k} \cdot \tau_m(t) = \sum_{n=1}^{nodes} [\gamma_m(t) \cdot \gamma_n(t) \ddot{\theta}_n(t) M_{m,n} - \gamma_m(t) \cdot \beta_n(t) (\dot{\theta}_n(t))^2 M_{m,n} + \gamma_m(t) \cdot \beta_n(t) K_{m,n}] \quad (1)$$

where  $\hat{k}$  is the z-axis unit vector,  $\tau_m$  is the applied torque at node  $m$ ,  $\gamma_m$  is a unit orthogonal vector at node  $m$ ,  $\theta_m$  is the inertial

## OPTIMAL TRAJECTORY PLANNING

As mentioned previously, minimum-time, straight line tip tracking error trajectories are considered. Constraints on these trajectories are: completing a rest-to-rest maneuver, tracking a specified path  $(x(t), y(t))_{tip}$ , slewing between specified endpoints  $[(x(t_0), y(t_0)), (x(t_f), y(t_f))]_{tip}$ , and not exceeding actuator torque limits,  $\pm \tau_{i,max}$ . End constraints on both velocities and accelerations are required to drive the flexible structure to rest at the final time  $t_f$ . Torque limits are incorporated naturally into the controls as

$$\tau_i = |\tau_{i,max}| \sin \alpha_i(t) \quad (2)$$

where  $\alpha_i(t)$  are free variables. Assuming the configuration initially starts at rest, the optimization problem can be stated as:

minimize:  $J = t_f$   
 subject to: --input actuator torques,  $\tau_i$   
 --the finite element model  
 --known initial conditions

constrained by:

$$C = \begin{bmatrix} x_{tip}(t_f) - x_{specified}(t_f) \\ y_{tip}(t_f) - y_{specified}(t_f) \\ \dot{\theta}_1(t_f) \\ \dot{\theta}_2(t_f) \\ \ddot{\theta}_1(t_f) \\ \ddot{\theta}_2(t_f) \\ \int_0^{t_f} [y_{tip}(x_{tip}(t)) - y_{line}(x_{tip}(t))]^2 dt \\ \tau_{1(max)} \\ \tau_{2(max)} \end{bmatrix} \quad (3)$$

where  $y_{tip}(x_{tip}(t))$  is the Y-axis coordinate of the second link tip corresponding to the X-axis tip coordinate at the current time,  $t$ . Note that the tip-tracking criteria includes an integral constraint for following the line and a point constraint for acquiring the end condition, while the constraints needed to bring the structure to rest are simply point constraints. No constraint is placed on link vibration during slew maneuvers and the structure is allowed to "ring" during the trajectory.

The hub and elbow optimized angle and torque histories from (Eisler, et. al., 1993) are shown in Figure 4 through Figure 6. The hub torque profile resembles the bang-coast-bang profile common to other minimum time, residual oscillation free maneuvers (Pettersen and Robinett, 1991; Parker, Robinett, Eisler, and Phelan, 1994). The elbow angle history is similar in form to a versine function ( $1 - \cos\Omega t$ ). This shape will be exploited later. Note that the elbow torque profile is near zero for most of the trajectory.

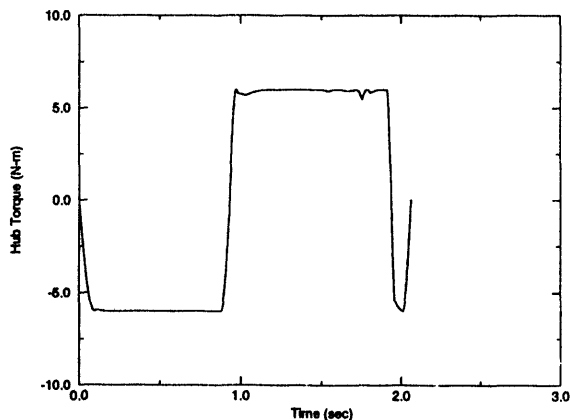


FIGURE 3. Hub Optimal Torque History

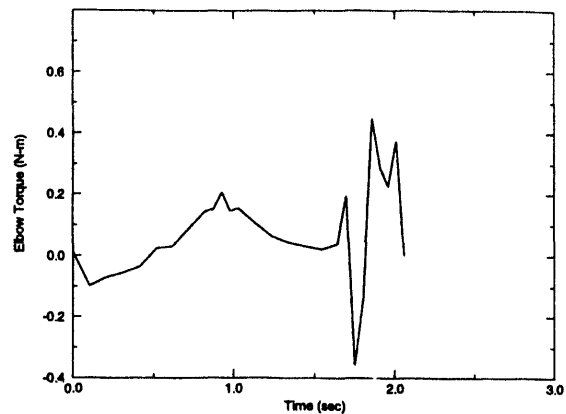


FIGURE 4. Elbow Optimal Torque History

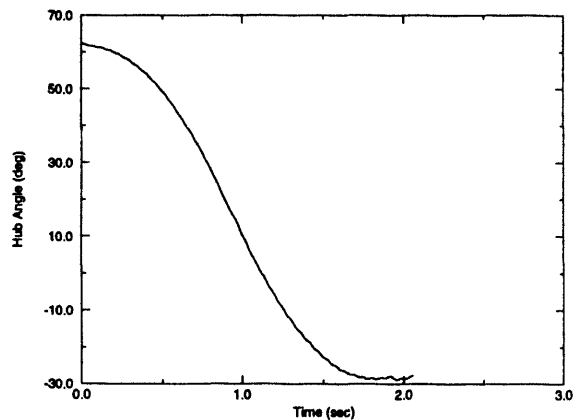


FIGURE 5. Hub Optimal Angle History

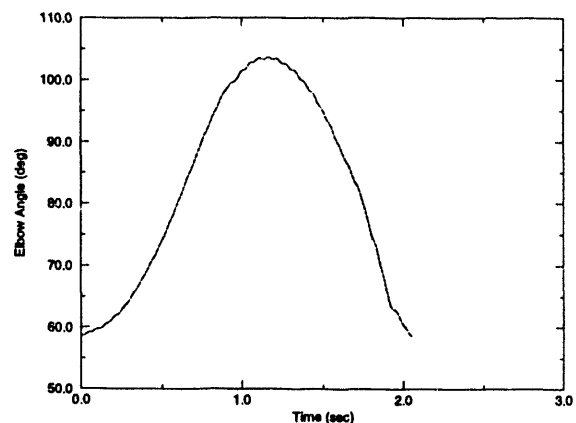


FIGURE 6. Elbow Optimal Angle History

## SERVO DYNAMICS AND INPUT COMMAND CONDITIONING

The joint actuators consist of D.C. motors and current regulating amplifiers. Under the assumption that current is proportional to motor torque, the actuators are torque following devices. As a first step to achieving the tracking objective, the joint torques, as calculated by the optimization process (Eisler, et. al.), are used as sole inputs to the current regulating amplifiers. The equation of motion describing the dynamics of this system are

$$J_m \ddot{\theta}_m + B_m \dot{\theta}_m = K_i i_a - \tau_L \quad (4)$$

where  $J_m$  is the motor inertia,  $B_m$  is the motor viscous friction damping,  $K_i$  is the motor torque constant,  $i_a$  is the motor armature current,  $\tau_L$  is the nonlinear load torque function imparted to the motors due to the motion of the links, including deformation degrees of freedom, and  $\theta_m$  is the joint angle. Because the dynamics of Eq. (4) are not included in the optimization process described in the previous section, the optimal torque (current) commands result in tracking errors in excess of 11 cm as shown in Figure 7.

The next step is to implement Proportional-Derivative (PD) servo loops at each joint's D.C. motor actuator. The control law at each joint takes the form

$$K_i i_a = K_p (\theta_c - \theta_m) + K_D (\dot{\theta}_c - \dot{\theta}_m) \quad (5)$$

where  $K_p$  is the proportional gain,  $K_D$  is the derivative gain, and  $\theta_c$  is the commanded joint angle. The equation of motion describing the dynamics of the servo controlled system are

$$J_m \ddot{\theta}_m + (B_m + K_D) \dot{\theta}_m + K_p \theta_m = K_D \dot{\theta}_c + K_p \theta_c - \tau_L \quad (6)$$

In this case the joint angle commands and joint angular velocity commands obtained from the optimization process are used as inputs to the servo controlled joint actuators. Once again, the performance of this method suffers from the lack of compensation of the dynamic effects in the commands resulting in maximum tracking errors of 13 cm as shown in Figure 7.

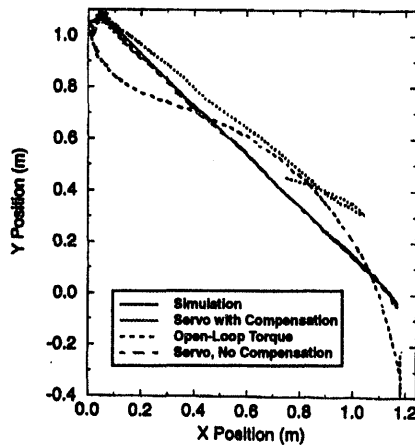


FIGURE 7. Comparison of Several Control Strategies for Straight Line Tracking

A systematic method is now developed for precompensating the desired joint angle commands thus creating inputs to the servo controlled joints to achieve accurate tracking. This precompensation method is trajectory dependant and therefore, may not be needed throughout an entire trajectory. For instance, for the two-link robot used here, specification of a hub trajectory yields a unique trajectory for the elbow joint due to inertial and frictional effects of the second link and joint. If that hub dependent motion of the elbow is the desired motion, then the elbow servo actuator would never be active. Precompensating the input commands to the elbow joint would result in deviations from the desired motion.

The first step of the procedure is to precompensate the hub joint input commands. This is accomplished by identifying an input/output relationship between joint commands and measured joint angles for the particular trajectory of interest during those portions of the trajectory where the actuator is active. Next, an inverse operator is obtained for this relationship. The joint servo actuator commands are obtained by applying the inverse operator to the desired joint history. Subsequent joint commands are precompensated in the same manner, where the current joint angle data is consistent with the inboard joint commands having been precompensated.

In the straight line tracking case considered here, the hub actuator is active throughout the entire trajectory. The form of the input/output relationship is postulated as

$$\frac{\theta_m}{\theta_c} = \frac{K(s + n_0)}{s^2 + d_1 s + d_0} \quad (7)$$

The desired hub trajectory is input to the servo actuator resulting in the encoder data of  $\theta_m$ . Obtaining an accurate input/output relationship is achieved by choosing the coefficients of Eq. (7) so as to minimize the integrated error between the filtered command history

$$\tilde{\theta}_m = \frac{K(s + n_0)}{s^2 + d_1 s + d_0} \theta_c \quad (8)$$

and the measured output joint history  $\theta_m$ . The identified coefficients of Eq. (7) are given in Table 2. Figure 8 shows the input commands, output encoder signal and the filtered command history  $\tilde{\theta}_m$  after completing the optimization process. Operating the inverse transfer function of Eq. (7) on the desired input commands for the hub gives the precompensated commands of Figure 9.

TABLE 2. Hub Transfer Function Values

Coefficient	Value
$K$	1.7211
$n_0$	2583.3
$d_1$	2081.5
$d_0$	4476.8

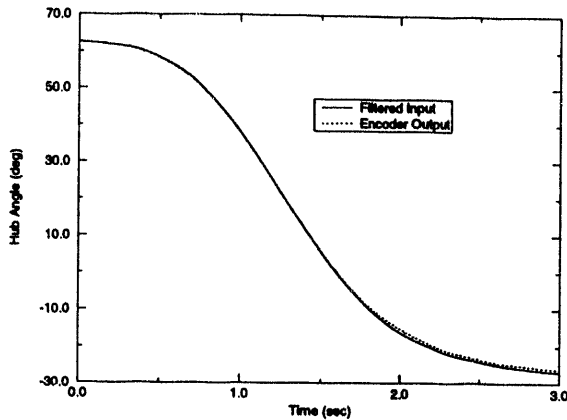


FIGURE 8. Filtered Input Commands Compared to Experimental Data for Verifying Accuracy of Hub Input/Output Operator

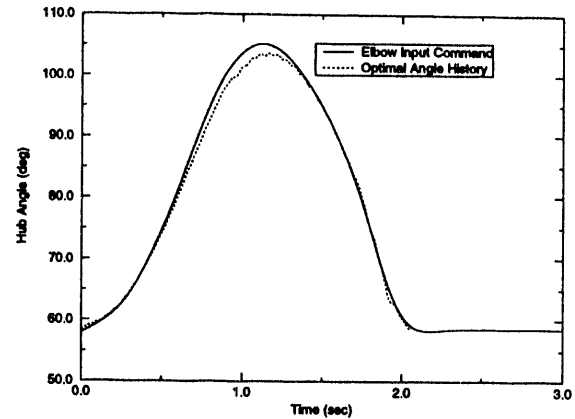


FIGURE 10. Joint Two Precompensated Command History

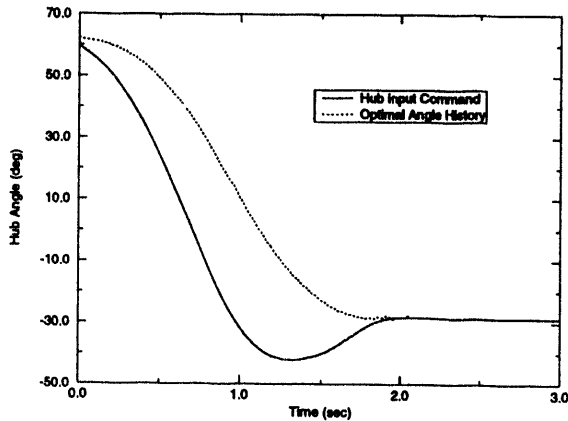


FIGURE 9. Joint One Precompensated Command History

The input commands to the elbow joint are obtained by precompensating the desired elbow trajectory only in the regions where a torque is required. From Figure 4 this corresponds to the portion of the trajectory between 0.8 and 1.0 seconds. Noting that the optimal angle of joint two resembles the versine function  $1 - \cos\Omega t$ , the inverse input/output operator is postulated as

$$\theta_c = K_2(1 - \cos\Omega[t - t_0])\theta_d \quad (9)$$

An iterative approach is used to obtain the best values for the design parameters  $K_2$ ,  $\Omega$ ,  $t_0$  shown in Table 3. The precompensated command for the elbow joint is shown in Figure 10.

TABLE 3. Joint Two Inverse Operator Values

Parameter	Value
$K_2$	0.006
$\Omega$	5.0
$t_0$	0.25

## RESULTS

The precompensated joint commands of Figure 9 and Figure 10 are used as inputs to the servo actuated joints. The joint encoder measurements indicated tracking of the desired joint angles to within 1.0 degrees as shown in Figure 11 and Figure 12. Furthermore, the straight line tracking error of less than 2.5 cm is better than that of the open loop torque input method and the servo actuator method without precompensation. These three methods are compared in Figure 7.

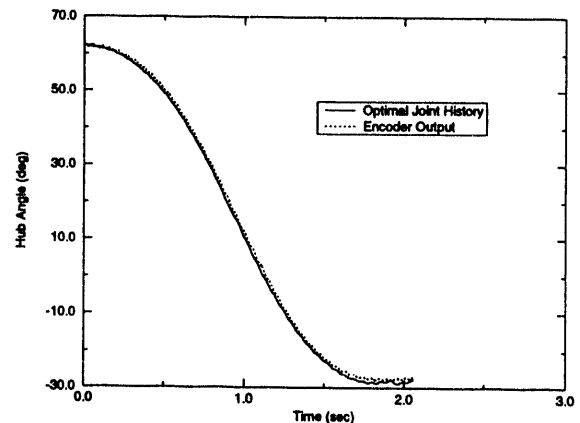


FIGURE 11. Joint One Comparison of Optimal History to Encoder Data

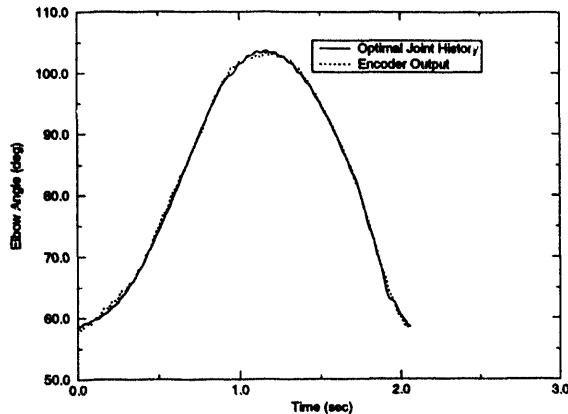


FIGURE 12. Joint Two Comparison of Optimal Joint History to Encoder Data

### SUMMARY

The focus of this work was to experimentally verify the analytical results of (Eisler, et. al.). In that work joint histories were calculated for a two-link flexible robot such that the tip of the second link tracked a straight line in minimum time and with no residual oscillation. When the joints of the experimental system, as measured via joint encoders, tracked those of the analytical study, the resulting maneuver was residual vibration free, thus verifying the results of (Eisler, et. al.).

In the process of verifying these results a systematic approach for precompensating joint input commands was developed and applied. This method relied on creating an input/output relationships between desired joint histories and measured joint angles. An inverse operator was then used to obtain the true servo actuator inputs to achieve the desired joint angle output history.

For the case where all joints of a multi-link system require torque throughout the trajectory, transfer functions can be used for the input/output relationships. Once obtained, the servo actuator commands can be obtained by reverse filtering the desired joint histories through the transfer functions. However, if the trajectories are such that some joints do not require external torque, then only those portions of the joint histories should be precompensated.

### REFERENCES

- Eisler, G. R., Robinett, R. D., Segalman, D. J., and Feddema, J. D., 1993, "Approximate Optimal Trajectories for Flexible-Link Manipulator Slewing Using Recursive Quadratic programming", ASME Journal of Dynamic Systems, Measurement, and Control, Vol 115, pp. 405-410.
- U.S. Department of Energy, "Environmental Restoration and Waste Management Robotics Technology Development Program Robotics 5-Year Program Plan", DOE/EM-0007T, Vol. 1-3, 1991.
- Mayes, R. L., 1001, "Experimental Characterization of Flexible Two Link Robot Arm", Internal Memorandum, Sandia National Laboratories.

Newmark, N. M., 1959, "A Method of Computation for Structural Dynamics", ASCE J. Eng. Mech. Div., Vol. 85, No. EM3, pp. 67-94.

Petterson, B. J., and Robinett, R. D., 1991, "Model-Based Damping of Coupled Horizontal and Vertical Oscillations in a Flexible Rod", J. of Intelligent and Robotic Systems, Vol. 4, pp. 285-299.

Parker, G. G., Eisler, G. R., Phelan, J. and Robinett, R. D., 1994, "Input Shaping for Vibration-Damped Slewing of a Flexible Beam Using a Heavy-Lift Hydraulic Robot", The 1994 American Automatic Control Conference.

### DISCLAIMER

This report was prepared as an account of work sponsored by an agency of the United States Government. Neither the United States Government nor any agency thereof, nor any of their employees, makes any warranty, express or implied, or assumes any legal liability or responsibility for the accuracy, completeness, or usefulness of any information, apparatus, product, or process disclosed, or represents that its use would not infringe privately owned rights. Reference herein to any specific commercial product, process, or service by trade name, trademark, manufacturer, or otherwise does not necessarily constitute or imply its endorsement, recommendation, or favoring by the United States Government or any agency thereof. The views and opinions of authors expressed herein do not necessarily state or reflect those of the United States Government or any agency thereof.

**DATE  
FILMED**

*10/13/94*

**END**

